# Radiative forcing by aerosols over the Bay of Bengal region derived from shipborne, island-based, and satellite (Moderate-Resolution Imaging Spectroradiometer) observations

V. Vinoj,[1] S. Suresh Babu,[2] S. K. Satheesh,[1] K. Krishna Moorthy,[2] and Y. J. Kaufman[3]

[1]   Measurements of spectral aerosol optical depths (AODs) were made over the Bay of Bengal region (adjacent to the Indian landmass) on board the oceanographic research vessel *Sagar Kanya* during February 2003. Simultaneous measurements of spectral AODs and mass concentrations of the composite aerosols and aerosol black carbon (BC) were made at an island location, Port Blair (11.63°N, 92.71°E), also in the Bay of Bengal. At the cruise locations the AODs were in the range of ∼0.3–0.6 at 500 nm (with a mean value of 0.41 ± 0.14) and Angstrom wavelength exponent of ∼1.1 ± 0.1; while at Port Blair the AODs were in the range of 0.11–0.48 at 500 nm and Angstrom wavelength exponent of 0.98 ± 0.07. Aerosol BC constituted 5.8 ± 0.6% of the composite aerosol mass concentration with a single-scattering albedo of ∼0.88, indicating the presence of a significant amount of submicron absorbing aerosols. Comparisons of AODs measured at Port Blair during cruise 188 and an earlier cruise (cruise 161B) during March 2001 (over the Bay of Bengal, Arabian Sea, and Indian Ocean) with those derived from Moderate-Resolution Imaging Spectroradiometer (MODIS) (on board the TERRA platform) showed excellent agreement with a mean difference of ∼0.01 and a root-mean-square difference of ∼0.03. Regionally averaged aerosol (net) forcing over the Bay of Bengal was in the range −15 to −24 W m$^{-2}$ at the surface and −2 to −4 W m$^{-2}$ at the top of the atmosphere in February 2003; these values were smaller in magnitude than those observed over this region during March 2001 and larger than that observed over the Arabian Sea and the Indian Ocean. The resulting atmospheric heating due to aerosol absorption was ∼0.5°K/d.    *INDEX TERMS:* 0305 Atmospheric Composition and Structure: Aerosols and particles (0345, 4801); 0345 Atmospheric Composition and Structure: Pollution—urban and regional (0305); 1640 Global Change: Remote sensing; 1610 Global Change: Atmosphere (0315, 0325); 1803 Hydrology: Anthropogenic effects; *KEYWORDS:* aerosols, radiative forcing, atmosphere

## 1.   Introduction

[2]   Recent investigations have demonstrated the importance of aerosols in Earth's radiation budget [*Charlson et al.*, 1991, 1992; *Bates et al.*, 1998; *Boucher et al.*, 1998; *Kaufman et al.*, 1998; *Haywood et al.*, 1999; *Russell et al.*, 1999; *Satheesh et al.*, 1999; *Subbaraya et al.*, 2000; *Satheesh and Ramanathan*, 2000; *Ramanathan et al.*, 2001; *Moorthy et al.*, 2001; *Kaufman et al.*, 2002]. Estimation of aerosol radiative forcing is more uncertain than the radiative forcing because of well-mixed greenhouse gases (GHGs), because of their short lifetimes and the highly heterogeneous spatial distribution. A description of aerosol forcing with comparable accuracies to that of GH forcing requires a better understanding of the aerosol size distribution, chemical composition, and vertical distribution and an accurate implementation of these relevant properties into radiative transfer and climate models [*Raes*, 1995; *Nemesure et al.*, 1995; *Boucher et al.*, 1998; *Boucher and Tanre*, 2000; *Soden et al.*, 2000; *Ansmann et al.*, 2002]. The current estimate of the globally averaged aerosol radiative forcing is comparable in magnitude (but of opposite sign) to the GHG forcing, but with much larger uncertainties [*Intergovernmental Panel on Climate Change (IPCC)*, 2001]. However, aerosol forcing can be even positive in regions where absorbing aerosols are present in sufficient amounts [*Coakley et al.*, 1983; *Coakley and Cess*, 1985; *Hansen et al.*, 1998; *Haywood et al.*, 1999]. Notwithstanding the potential climate impact of aerosols, they are poorly characterized

[1]Centre for Atmospheric and Oceanic Sciences, Indian Institute of Science, Bangalore, India.
[2]Space Physics Laboratory, Vikram Sarabhai Space Centre, Thiruvananthapuram, India.
[3]Climate and Radiation Branch, NASA Goddard Space Flight Center, Greenbelt, Maryland, USA.

in climate models because of the lack of a comprehensive database. Comprehensive observations conducted during Indian Space Research Organization's Geosphere Biosphere Programme (ISRO-GBP) and Indian Ocean Experiment (INDOEX) have resulted in a reasonably good amount of information on aerosols over the Indian subcontinent, Indian Ocean and Arabian Sea [*Subbaraya et al.*, 2000; *Moorthy et al.*, 2001; *Ramanathan et al.*, 2001]. The results from the above experiments demonstrated the importance of aerosols over this region on the radiation budget and regional climate. However, none of these experiments have made measurements over the Bay of Bengal until 2001 even though aerosol radiative forcing over the Bay of Bengal has an important role in regional climate system. A good part of the rainfall associated with Indian monsoon is generated by the westward moving depressions or low-pressure systems in the Bay of Bengal [*Das*, 1986; *Asnani*, 1993].

[3] In this paper, we report the results of measurements of aerosol spectral optical depths (AODs) made over the Bay of Bengal region on board the oceanographic research vessel *Sagar Kanya* during its cruise 188 during February 2003. Simultaneously with these measurements, measurements of spectral AODs and mass concentrations of the composite aerosols and aerosol black carbon (BC) were made at an island location, Port Blair (11.63°N, 92.71°E), located farther east in Bay of Bengal [*Moorthy et al.*, 2003]. These AODs were compared with the corresponding Moderate-Resolution Imaging Spectroradiometer (MODIS) (on board the TERRA platform) AODs, at the near-infrared wavelength (865 nm), providing the first-time intercomparison of MODIS derived AODs with those measured from ground over this region. These observations are integrated to estimate the regionally averaged aerosol radiative (shortwave and longwave) forcing over the Bay of Bengal region. The results are examined in light of available knowledge from previous experiments such as ISRO-GBP and INDOEX and the implications are discussed.

## 2. Instrumentation and Data

### 2.1. Aerosol Optical Depths

[4] The investigations were made over the Bay of Bengal (BoB) (1) on board the Oceanographic Research Vessel ORV *Sagar Kanya* during its cruise 188 from 18 to 28 February 2003 and (2) simultaneously from the island location, Port Blair. The details of the cruise tracks and the location of the island with respect to the Indian mainland are shown in Figure 1. The onboard measurements were limited to spectral AODs, made using a multispectral handheld Microtops Sun photometer (Solar Light, United States). It provided AODs at 5 channels (340, 380, 500, 675, and 870 nm) derived from instantaneous solar flux measurements using its internal calibration. A Global Positioning System (GPS) receiver attached with the photometer provided the information on time, location, altitude and pressure. More details are available elsewhere [*Morys et al.*, 2001; *Porter et al.*, 2001; *Ichoku et al.*, 2002a].

[5] Spectral AODs at Port Blair were estimated using a 10-channel multiwavelength solar radiometer (MWR) located on the rooftop of the observatory, set up in 2002 (see *Moorthy et al.* [2003] for details) at 10 wavelengths (380,
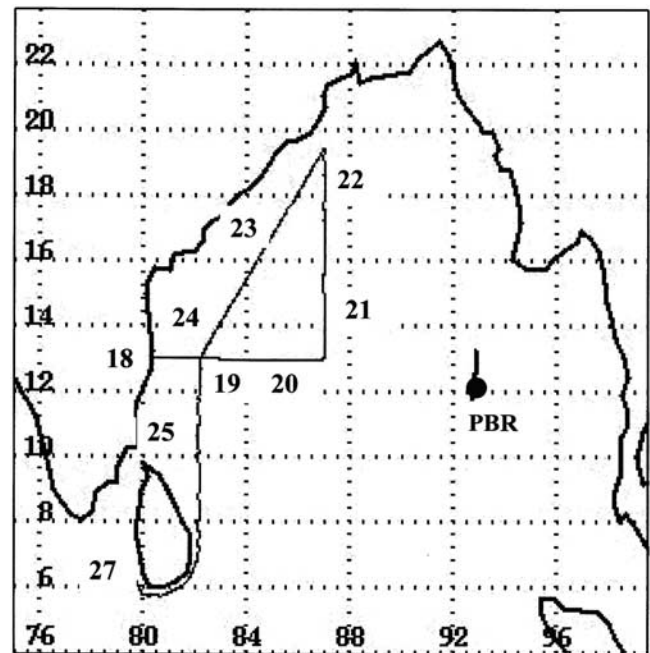


**Figure 1.** Cruise track of R/V *Sagar Kanya* cruise 188 during February 2003. The numbers on the track represent the date in February, and PBR represents location of Port Blair island site.

400, 450, 500, 600, 650, 750, 850, 935, and 1025 nm). More details on the MWR including analysis details and error budget are given in several earlier papers [*Satheesh and Moorthy*, 1997; *Moorthy et al.*, 1997, 1999, 2001].

### 2.2. Composite and BC Aerosol Mass Concentration

[6] In addition to spectral AODs, simultaneous measurements of mass concentration of composite aerosols and aerosol black carbon (BC) were made from Port Blair. Estimates of BC aerosols were made using an aethalometer; model AE-21 of Magee Scientific, United States [*Hansen et al.*, 1984; *Hansen*, 1996; *Babu and Moorthy*, 2001, 2002]. The instrument was operated at a flow rate of 4 L min$^{-1}$ and at a time-base of 5 min. More details on the operation of the aethalometer and its error budget are available elsewhere [*Babu and Moorthy*, 2002]. Near-simultaneous measurements of the composite aerosol mass concentration were made using a 10-channel quartz crystal microbalance (QCM) impactor (PC-2 of California measurements), which made periodic samples at a sampling interval of 5–8 min at a flow rate of 240 mL/min. More details on the measurement technique, precautions involved and error budget are given by *Pillai and Moorthy* [2001].

[7] In addition to these data obtained during February 2003, we have used the data from an earlier cruise (cruise 161B) carried out in March 2001 over BoB, Indian Ocean and Arabian Sea surrounding Indian Peninsula [*Satheesh et al.*, 2001; *Satheesh*, 2002] in which spectral AODs were obtained using an EKO Sun photometer (EKO Inc., Japan). Intercomparison of the AODs estimated using all the three instruments at the common wavelength (500 nm) has shown a fairly good agreement with a root-mean-square difference of less than 0.02 to 0.05 [*Satheesh et al.*, 2001].
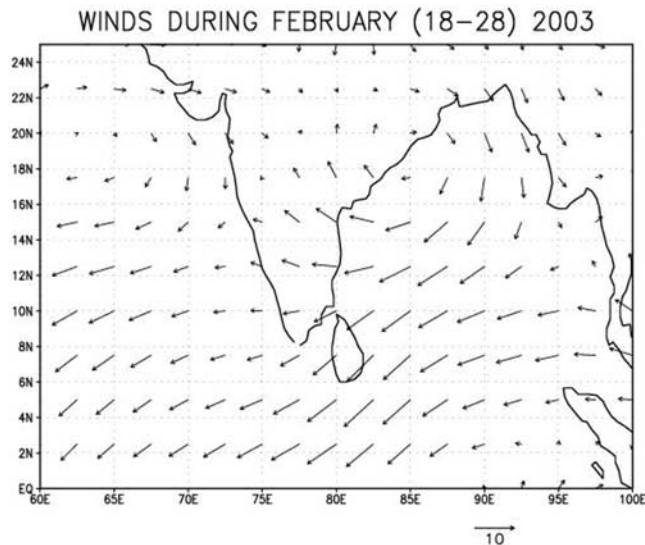
**Figure 2.** Synoptic wind pattern during the cruise period (using NCEP data).

[8] In addition to all these ground-based measurements, we have also used AODs from MODIS (Level 3 data) (on board the TERRA platform) as well in the present study.

### 2.3. Meteorology

[9] The synoptic meteorological conditions during the cruise period were quite similar to those known to prevail over the oceanic regions adjacent to the Indian subcontinent during February/March [*Das*, 1986; *Asnani*, 1993; *Moorthy et al.*, 1999, 2003; *Moorthy and Satheesh*, 2000]. The wind pattern during the cruise period is shown in Figure 2 (using National Center for Environmental Prediction (NCEP) data). Over Bay of Bengal northwesterly winds prevailed, directed from the east coast of India. The major industries in regions upwind of the study area (Bhubaneswar, Kolkatta, Visakhaptnam, etc.) include cement factories, thermal power plants (coal based), steel plants, etc. [*Satheesh*, 2002]. Detailed analyses on wind pattern (on a daily basis) (using NCEP data) and back trajectory analysis using Hybrid Single-Particle Lagrangian Integrated Trajectory (HYSPLIT4) Model at different locations in Bay of Bengal have shown that during the study period (i.e., February 2003), Bay of Bengal was influenced by air masses from east coast and central India for more than 70% of the time. Typical back trajectories are shown in Figure 3a for central BoB and Figure 3b for Port Blair. The details of trajectories at three different altitudes levels considered in this study [marine atmospheric boundary layer (MABL), above the MABL but below the trade-wind inversion and in the lower free-troposphere] are given in Table 1 on a daily basis. Thus results reported in this paper are representative of the winter season; i.e., when air mass is from the Indian subcontinent during most of the season. Figure 2 shows that during the cruise period, Port Blair was often influenced by oceanic air masses (from the southeast).

### 3. Results and Discussion

#### 3.1. Aerosol Optical Depths

[10] Aerosol optical depths ($\tau_a$) obtained from cruise 188 are shown in Figure 4a at four representative wavelengths.
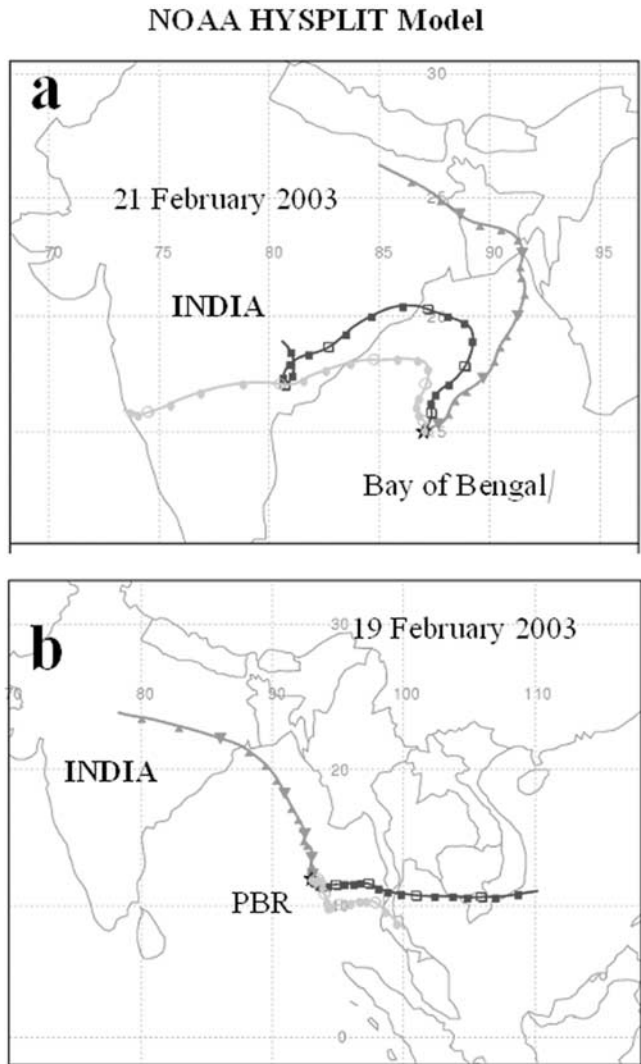


**Figure 3.** A typical example of air mass trajectory (a) over the Bay of Bengal during the cruise period at three different altitudes (circles represent 500 m, squares represent 1500 m, and triangles represent 2500 m) and (b) at Port Blair.

**Table 1.** Origin and Trajectory of Air Masses Encountered During the Experiment[a]

| Date in February 2003 | Port Blair | | | Bay of Bengal | | |
|---|---|---|---|---|---|---|
| | 500 m | 1500 m | 2500 m | 500 m | 1500 m | 2500 m |
| 19 | CI, EI | EA | EA | CI, EI | WA, CI, EI | WA, CI, EI |
| 20 | EA | EA | WA, CI, EI | CI, EI | CI, EI | CI, EI |
| 21 | EA | EA | EI | CI, EI | CI, EI | CI, EI |
| 22 | OC | OC | CI, EI | CI, EI | WA, CI, EI | WA, CI, EI |
| 23 | CI, EI | OC | CI | CI, EI | WA, CI, EI | WA, CI, EI |
| 24 | CI, EI | OC | EI | CI, EI | CI, EI | CI, EI |
| 25 | WA, CI, EI | OC | WA, CI, EI | CI, EI | CI, EI | CI, EI |
| 26 | WA, CI, EI | EI | EI | CI, EI | CI, EI | CI, EI |
| 27 | CI, EI | OC | OC | EI | CI, EI | WA, CI, EI |
| 28 | CI, EI | EA | EA | CI, EI | WA, CI, EI | CI, EI |

[a]CI, Central India; EI, Eastern India; OC, Oceanic; EA, East Asia; WA, West Asia.
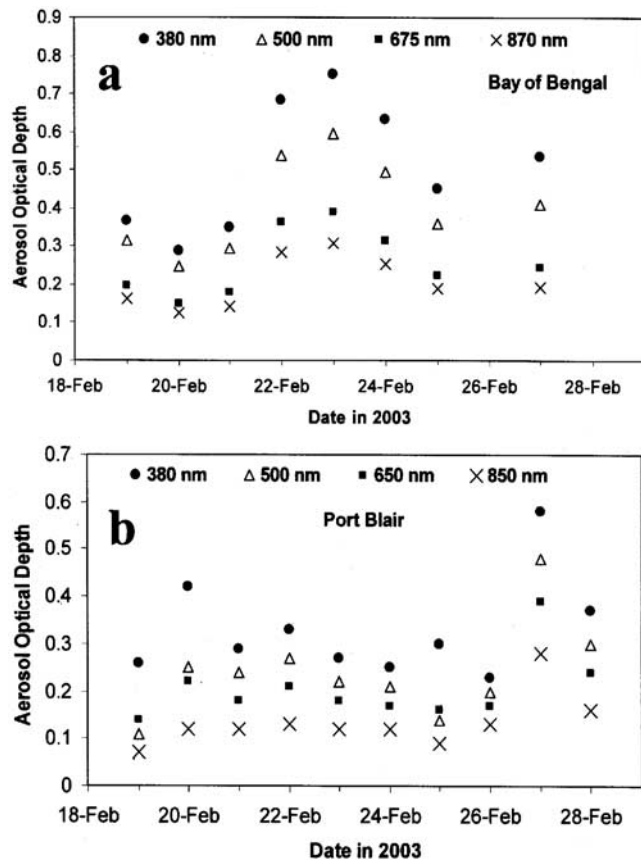
**Figure 4.** Aerosol optical depths at four wavelengths (a) during the cruise and (b) at Port Blair.



**Figure 5.** Average spectral optical depths at Port Blair Island in the Bay of Bengal during the cruise period.

Simultaneous measurements at Port Blair are shown in Figure 4b. Measurements were made when the sky was free of visible clouds or when clouds were far away from the solar disk. Additional precautions were also taken while making Microtops observations from the ship [*Morys et al.*, 2001; *Ichoku et al.*, 2002a]. This was not difficult as wind speed was less than 5 m s$^{-1}$ for most of the observation period. It can be seen that $\tau_a$ at 500 nm was ~0.3 over regions away from the coast, and when the ship approached the east coast of India on 22–24 February, $\tau_a$ values have increased to ~0.6. The aerosol optical depth at 500 nm averaged for the entire cruise is 0.41 ± 0.14. Corresponding values for other wavelengths are given in Table 2. Since we have observed an increase in $\tau_a$ at 500 nm over the near coastal oceanic regions compared to far oceanic regions (at least 300 km away from the coast), we have estimated near coastal and far oceanic optical depth averages, and these are shown in Table 2. It can be seen that optical depths over oceanic regions near the coast are higher (with $\tau_a$ value of
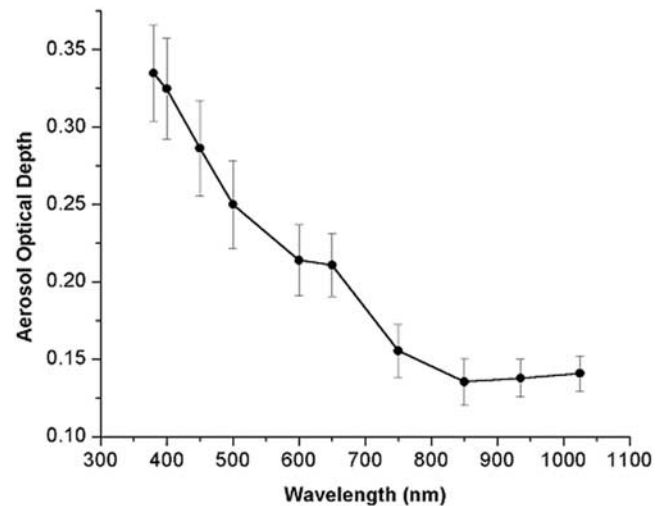
0.54 ± 0.05) compared to the open ocean (0.30 ± 0.05). On the other hand, AODs at Port Blair were generally lower, with AOD at 500 nm in the range of 0.1 to 0.48 with a mean value of 0.25 ± 0.03. The spectral variation of the mean AOD at Port Blair is shown in Figure 5, where the vertical bars represent standard deviation of the mean. It can be seen that the AODs at all wavelengths are significantly lower at Port Blair compared to even far oceanic regions of the cruise. This could be due to different air masses influencing the two locations or the long sea-travel of the air masses from the source regions as seen from Figure 2 and Table 1.

### 3.2. Comparison With MODIS-Derived AODs

[11] As can be seen from Figure 1, the cruise was limited to a relatively small oceanic region, while the island observations were from a fixed location. However, oceanic regions, particularly those adjacent to densely inhabited continents and under the influence of varying continental air mass, are known to show spatial heterogeneity even within a given season [*Satheesh*, 2002; *Sakerin and Kabanov*, 2002]. Thus for drawing conclusions on regional impacts based on such limited region measurements, it is essential to use satellite-derived observations, which have been validated/compared with the ground-based measurements. With a view to attaining AOD distribution over Bay of Bengal, we have used MODIS-derived AODs [*Ichoku et al.*, 2002b; *Remer et al.*, 2002; *Kaufman et al.*, 2003]. We have compared the AODs derived from the MODIS (at 865 nm at which ocean is a dark target) with the AODs estimated using the MWR (at 850 nm) and the Microtops (at

**Table 2.** Mean AODs and Angstrom Parameters Over BoB During February 2003

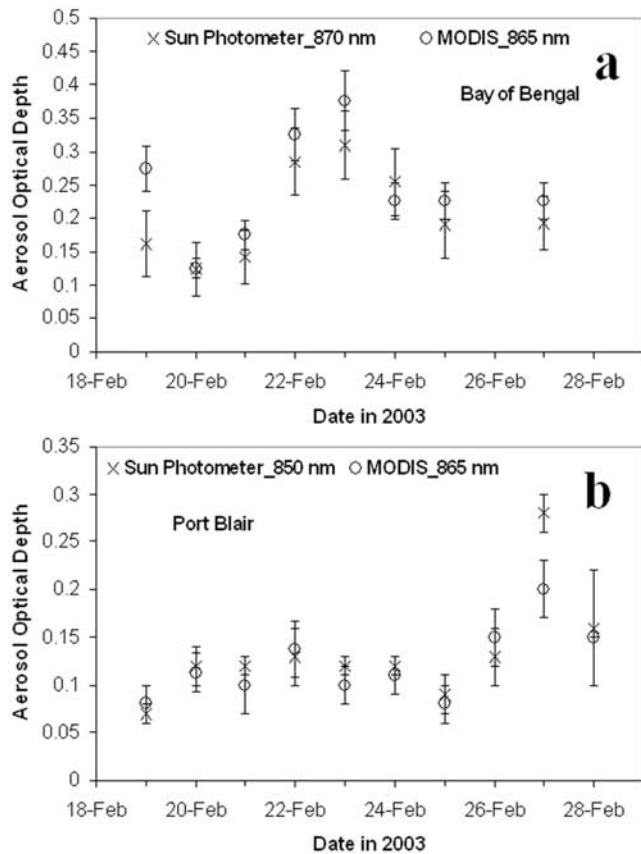| | Aerosol Optical Depth at λ, μm | | | | Angstrom Exponents | |
|---|---|---|---|---|---|---|
| Location | 0.38 | 0.5 | 0.675 | 0.87 | α | β |
| Cruise region | 0.50 ± 0.18 | 0.41 ± 0.14 | 0.26 ± 0.10 | 0.21 ± 0.07 | 1.1 | 0.18 |
| Near coastal | 0.69 ± 0.06 | 0.54 ± 0.05 | 0.36 ± 0.04 | 0.28 ± 0.03 | 1.12 | 0.24 |
| Far coastal | 0.36 ± 0.07 | 0.30 ± 0.05 | 0.19 ± 0.03 | 0.15 ± 0.03 | 1.1 | 0.13 |

**Figure 6.** Comparison of Sun photometer optical depths and MODIS optical depths on a day-to-day basis. (a) Bay of Bengal and (b) Port Blair.

870 nm). The comparison for the observational period is shown in Figure 6a for cruise locations and in Figure 6b for Port Blair. A good agreement is seen in both cases, with the values agreeing well within the instrumental uncertainties. To extend the validation, we have used AOD data collected during an earlier cruise in March 2001 over BoB, Indian Ocean and Arabian Sea (for details, see *Satheesh* [2002]). A scatterplot of the AODs from ground-based measurements with the corresponding values derived from the MODIS data is shown in Figure 7. The horizontal bars are the standard deviation of the Sun photometer optical depths where as vertical bars are the standard deviation of the $1° \times 1°$ pixel averaged AOD from MODIS at the ship location ($2° \times 2°$ for Port Blair) on the corresponding day. The solid line represents the ideal case. This combined database also helped in increasing the sample size as well as to check the consistency of the validation over a longer period of time. It can be seen from Figure 7 that the agreement is very good with a mean difference of $\sim 0.01$ and root-mean-square difference of $\sim 0.03$. This agreement provides the first-time intercomparison of the MODIS data with ground-based measurements over the oceanic regions adjacent to the Indian region. This enabled us to extrapolate our measurements over the BoB region by interlacing with the MODIS-derived AOD values. A least squares fit between AODs from the two estimates shows a linear relationship of the form AOD(MODIS) = AOD(SP) * 0.86 + 0.03, where

AOD(SP) is the Sun photometer derived optical depths and AOD(MODIS) is optical depth derived from MODIS.

### 3.3. Regional Distribution of AOD Over the Bay of Bengal

[12] The regional distributions of AOD at 865 nm over BoB, Arabian Sea and Indian Ocean during March 2001 and February 2003 derived from MODIS data are shown respectively in Figures 8a and 8b. The corresponding maps for 550 nm are shown in Figures 9a and 9b including Indian landmass. Notwithstanding the high values seen in March 2001 compared to February 2003, the spatial distribution remains nearly similar over this region in both observation periods. The average aerosol optical depth at 850 nm observed at Port Blair during the cruise period is 0.12 ± 0.02. It can be seen that MODIS optical depths agree with this (0.12 ± 0.02 averaged over $2° \times 2°$ around Port Blair) (Figure 8b). The same is true at 550 nm also as can be seen from Figures 5 and 9b. The average aerosol optical depths (and the number of observations) observed during cruise and regional average values (MODIS) for different seasons and locations together with observed values at Port Blair (Bay of Bengal, March 2001; Bay of Bengal, February 2003; Port Blair, February 2003; Arabian Sea, March 2001; and Indian Ocean, March 2001) are shown in Table 3. The difference between the two is not surprising as this could be due to the fact that the cruise measurements do not represent the entire oceanic region. Moreover, the agreement appears to be better when compared with the measurements from a fixed platform (island) than with the cruise.

### 3.4. Spectral Variation of AODs

[13] Spectral AODs contain information pertaining to aerosol size distribution. Following the inverse power law representation of the spectral variation of aerosol optical depth of *Angstrom* [1964],

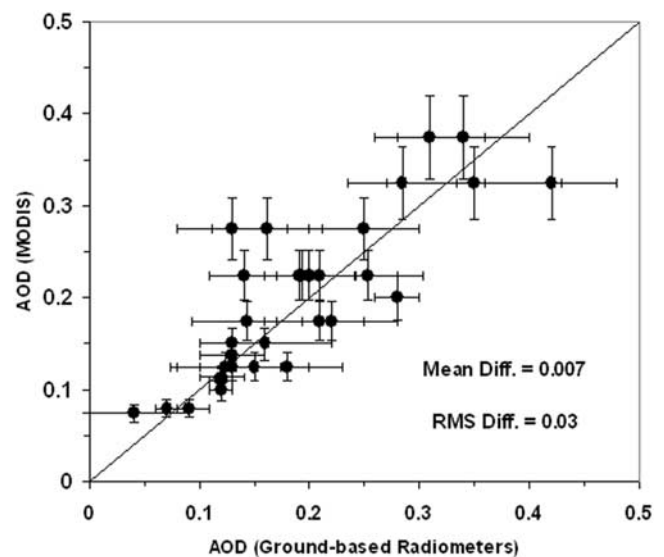$$\tau_a = \beta\lambda^{-\alpha}, \qquad (1)$$



**Figure 7.** Scatterplot of Sun photometer optical depths and MODIS optical depths.
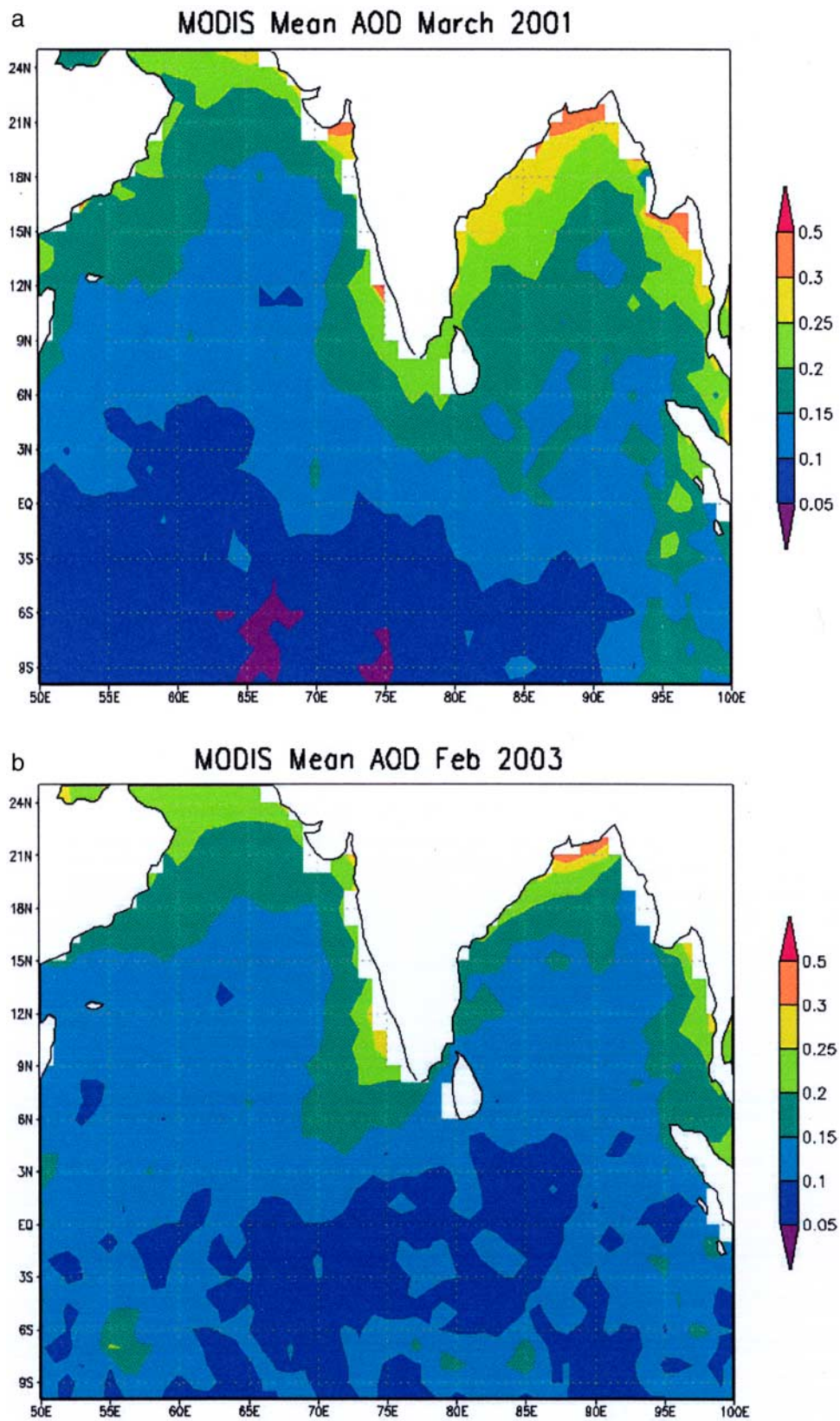
**Figure 8.** Regional distribution of aerosol optical depth (865 nm) during (a) March 2001 and (b) February 2003.
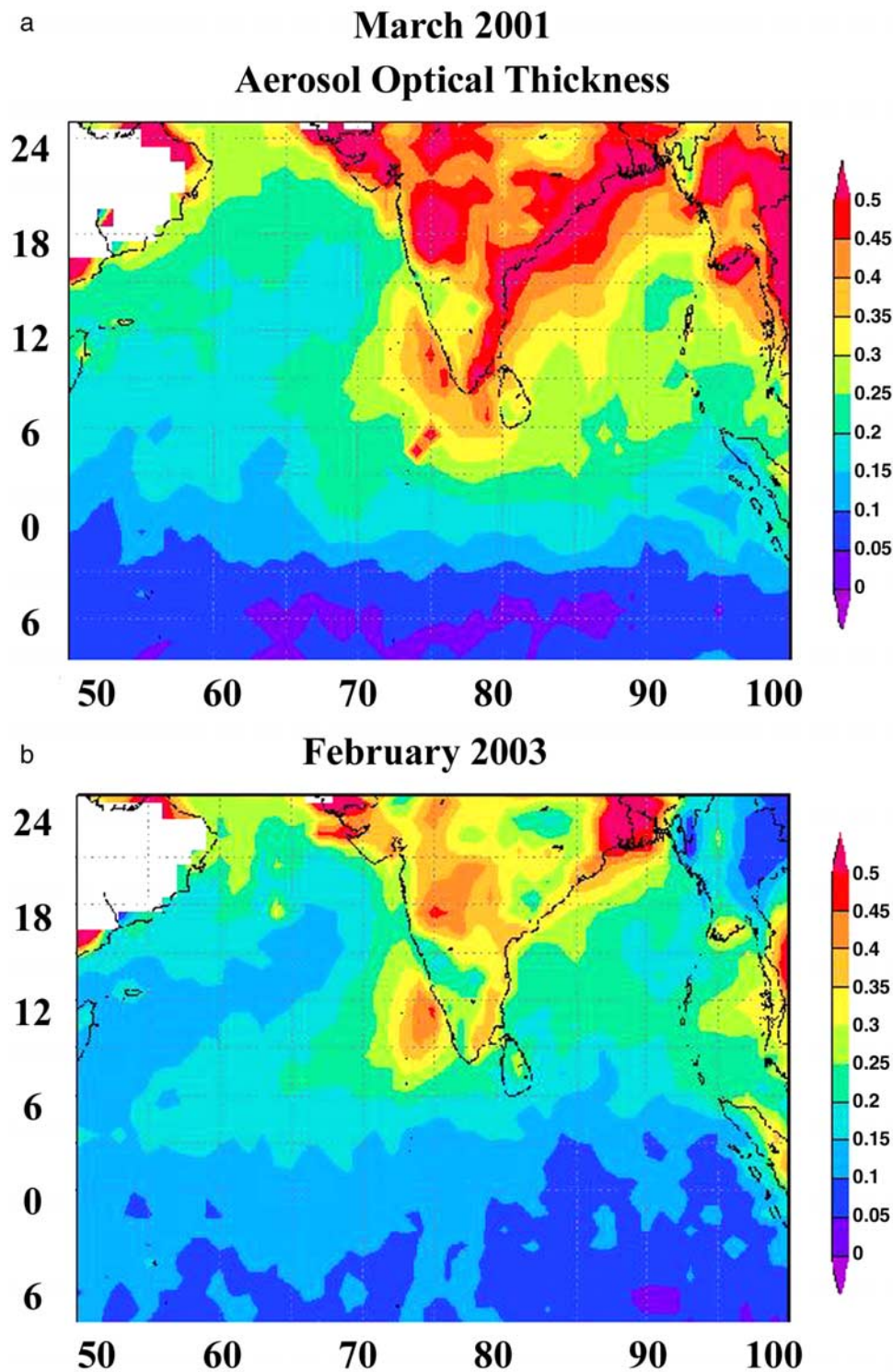
**Figure 9.** Regional distribution of aerosol optical depth (550 nm) during (a) March 2001 and (b) February 2003 (http://lake.nascom.nasa.gov/movas).

where $\alpha$ is the wavelength exponent, $\beta$ is the turbidity parameter and $\lambda$ is the wavelength in $\mu m$. The value of $\alpha$ depends on the ratio of the concentration of large to small aerosols and $\beta$ represents the total aerosol loading in the atmosphere [*Shaw et al.*, 1973]. For the case where the aerosol number size distribution follows inverse power law form

$$n(r) = n_0 r^{-\gamma}, \tag{2}$$

**Table 3.** Comparison of Sun Photometer Measured and Regional Mean MODIS AODs

| Location and Season | N,[a] days | Sun Photometer/MWR AOD (870/850 nm) | MODIS AOD (865 nm) (Regional Mean) | Sun Photometer/MWR AOD (500 nm) | MODIS AOD (550 nm) (Regional Mean) |
|---|---|---|---|---|---|
| Bay of Bengal, March 2001 | 6 | 0.19 ± 0.07 | 0.21 ± 0.09 | 0.44 ± 0.19 | 0.38 |
| Bay of Bengal, February 2003 | 8 | 0.21 ± 0.07 | 0.17 ± 0.08 | 0.41 ± 0.14 | 0.24 |
| Port Blair, February 2003 | 8 | 0.12 ± 0.02 | 0.12 ± 0.02 | 0.25 ± 0.03 | 0.22 (10° × 10° box) |
| Arabian Sea, March 2001 | 7 | 0.17 ± 0.06 | 0.17 ± 0.07 | 0.35 ± 0.19 | 0.27 |
| Indian Ocean, March 2001 | 6 | 0.17 ± 0.02 | 0.11 ± 0.05 | 0.21 ± 0.03 | 0.23 |

[a]Number of AOD observations during each day is typically 15–20.

where n(r) is the number concentration of aerosols in an infinitesimal radius dr centered at r, $n_0$ is a constant depending on the total aerosol concentration and $\gamma$ is the power-law index, $\alpha$ and $\gamma$ are related through the expression

$$\gamma = \alpha + 3. \qquad (3)$$

Higher values of $\alpha$ thus indicate a sharper aerosol size spectrum, more dominated by smaller aerosols. The values of $\alpha$ and $\beta$ are obtained by linear least squares fitting of $\tau_{a\lambda} - \lambda$ estimates on a log-log scale. The values of $\alpha$ and $\beta$ over Bay of Bengal are given in Table 2.

[14] Higher dominance of small particles is observed over Bay of Bengal as indicated by the higher values of $\alpha(\sim 1.1)$. While the value of $\alpha$ was $0.99 \pm 0.06$ at Port Blair, over the remote Indian Ocean sector its value is less than half the value over the Bay of Bengal [Satheesh, 2002; Moorthy et al., 2003]. This indicates that the fine submicron aerosols contributing to $\tau_a$ at shorter wavelengths are more of continental origin and dominate over the oceanic regions of east coast of India. The size distributions of aerosols over the Arabian Sea and Indian Ocean have been studied in detail by Moorthy et al. [1998]. Also in a simple way (using the Angstrom parameters) the size characteristics over the Arabian Sea are reported by Satheesh and Moorthy [1997]. The value of $\alpha$ reported by them for the Arabian Sea range from 1.2 for near coastal regions to 0.6 in remote oceanic regions. In the present study, though the value of $\alpha$ for near coastal regions of Bay of Bengal is $\sim 1.1$ (Table 2), it does not decrease even at Port Blair, lying more than 1500 km from the mainland. The large values of AODS and $\alpha$ over Bay of Bengal region could be due to the direct anthropogenic impact.

### 3.5. Radiative Forcing

[15] As the data on aerosol chemical properties were not available over this region, we have used aerosol models of Hess et al. [1998]. To describe a wide range of possible aerosol compositions, Hess et al. [1998] modeled aerosols as various components, each of them meant to be representative for a certain origin. These components can be mixed together to form various aerosol mixtures (such as continental clean, marine polluted etc). The value of $\alpha$ over Bay of Bengal suggests that the aerosols over this region are similar to the "marine polluted aerosol" model of Hess et al. [1998]. The components of marine aerosol model are sea salt, soot (BC), sulphate, and mineral dust. From the simultaneous measurements of composite aerosol mass concentration using the Quartz Crystal Microbalance (QCM; model PC2 of California Measurements, United States) and aerosol black carbon (BC) mass concentration

at Port Blair, the mass fraction of BC to composite aerosol is estimated by making a scatterplot of the two and obtaining the slope of the least squares fitted line through the origin [e.g., Babu et al., 2002]. The BC mass fraction thus estimated is $\sim 5.8 \pm 0.6\%$. This is quite similar to the BC fraction of $\sim 6\%$ reported for tropical Indian Ocean during INDOEX [Satheesh et al., 1999].

[16] In order to make the model consistent with observations, the number densities of individual components (in marine polluted aerosol model) are adjusted so as to make the BC mass fraction, aerosol optical depth at 500 nm and the value of $\alpha$ consistent both in observations and model. This approach of mixing various aerosol components is described in detail by Satheesh [2002], Babu et al. [2002], and Satheesh and Srinivasan [2002]. Following this approach, a simple aerosol model was derived for Bay of Bengal following the above papers as well as Satheesh et al. [1999] and Satheesh [2002]. The physical (mode radii, standard deviation, density etc) and optical properties (single-scattering albedo) of the individual aerosol components are shown in Table 4 [Hess et al., 1998]. In Table 4, $r_m$ is the mode radius and $\sigma_m$ is the standard deviation of the lognormal size distribution function. The aerosol single-scattering albedo of the composite aerosol is the average of individual species single-scattering albedo weighted by the corresponding extinction coefficients [Satheesh et al., 1999; Satheesh and Ramanathan, 2000]. The single-scattering albedo ($\omega$) thus estimated for Bay of Bengal is $\sim 0.88$.

[17] The above values of $\omega$ along with aerosol spectral optical depths and Angstrom wavelength exponent are incorporated in a Discrete Ordinate Radiative Transfer model (Santa Barbara DISORT Atmospheric Radiative Transfer (SBDART) model) to estimate the shortwave and longwave (clear sky) aerosol radiative forcing at the surface and top of the atmosphere (TOA). This model is designed and developed by University of California, Santa Barbara [Ricchiazzi et al., 1998], and is based on a collection of well-tested and reliable physical models, which were developed by the atmospheric science community over the past few decades. The estimated aerosol radiative forcing

**Table 4.** Physical and Optical Properties of Different Aerosol Species

| Aerosol Component | $r_m$, μm | $\sigma_m$ | $\rho$, g cm$^{-3}$ | $R_{eff}$, μm | $\omega$ |
|---|---|---|---|---|---|
| Water soluble (sulphate, nitrate, organics) | 0.029 | 2.24 | 1.8 | 0.165 | 0.99 |
| Soot | 0.018 | 2.0 | 1.0 | 0.065 | 0.23 |
| Sea salt (accumulation mode) | 0.378 | 2.03 | 2.2 | 2.5 | 1.0 |
| Sea salt (coarse mode) | 3.17 | 2.03 | 2.2 | 2.5 | 1.0 |
| Mineral dust | 0.39 | 2.0 | 2.6 | 1.9 | 0.82 |

**Table 5.** Regionally Averaged Aerosol Forcing[a]

| Location and Season | TOA | | | Surface | | |
|---|---|---|---|---|---|---|
| | SW | LW | Net | SW | LW | Net |
| Bay of Bengal, March 2001 | −5.9 (−6.9) | +2.5 (+2.9) | −3.4 (−4.0) | −33.7 (−39.1) | +9.8 (+11.4) | −23.9 −(27.7) |
| Bay of Bengal, February 2003 | −3.8 (−6.3) | +1.6 (+2.7) | −2.2 (−3.6) | −20.4 (−34.2) | +5.8 (+9.8) | −14.6 (−24.4) |
| Arabian Sea, March 2001 | −5.9 (−7.6) | +1.7 (+2.2) | −4.2 (−5.4) | −18.9 (−24.5) | +6.4 (+8.3) | −12.5 (−16.2) |
| Indian Ocean, March 2001 | −6.8 (−6.2) | +1.2 (+1.1) | −5.6 (−5.1) | −10.1 (−9.2) | +4.3 (+3.9) | −5.8 (−5.3) |

[a]Values are given in W m$^{-2}$. The values inside parentheses represent aerosol forcing estimated using average AOD from cruises.

(regionally averaged) is given in Table 5 and Figures 10a and 10b. For March 2001 we have used the aerosol models reported by *Satheesh* [2002] for estimating the radiative forcing.

## 4. Implications

[18] In the following, we examine our results and inferences in the light of the current understanding of aerosols and their regional radiative effects, particularly over oceanic environments.

[19] The net atmospheric forcing indicates the amount of radiative flux absorbed by the atmosphere due to the presence of aerosols. This energy is converted into heat. The resulting atmospheric heating rate can be calculated [*Liou*, 1980].

$$\frac{\partial T}{\partial t} = \frac{g}{c_p} \frac{\Delta F}{\Delta P},\qquad(4)$$

where $\partial T/\partial t$ is the heating rate (s$^{-1}$), g is the acceleration due to gravity, $C_p$ the specific heat capacity of air at constant pressure ($\sim$1006 J kg$^{-1}$ K$^{-1}$) and P is the atmospheric pressure, respectively. The atmospheric absorption observed in the present study thus translates into a heating rate of $\sim$0.5 K d$^{-1}$ when a value of 300 hPa is considered for $\Delta$P.

[20] A detailed compilation of aerosol optical depths over oceans by *Smirnov et al.* [2002] shows that the aerosol optical depths over the Arabian Sea during winter monsoon season are comparable to those reported for oceanic regions adjacent to industrialized continents. Measurements as part of TARFOX over the Atlantic Ocean in the haze plume off the east coast of United States have shown aerosol optical depths (at 500 nm) exceeding 0.5 (with mid-visible single-scattering albedo of $\sim$0.9) [*Russell et al.*, 1999; *Smirnov et al.*, 1995, 2000]. Also, *Smirnov et al.* [2002] have reported aerosol optical depth values as high as $\sim$0.7 during dry season over Persian Gulf with an annual average of $\sim$0.25. Using AVHRR data, *Li and Ramanathan* [2002] have reported that the maximum in aerosol optical depth over the Arabian Sea occurs in July (with $\tau_a \sim 0.6$) and minimum in January (with $\tau_a \sim 0.2$). Similar results are also reported by *Eck et al.* [2001]. Measurements during SCAR-B have shown that at the TOA, the shortwave aerosol forcing efficiency (forcing per unit aerosol optical depth) was in the range −20 to −60 W m$^{-2}$ [*Christopher et al.*, 2000, 2002]. Using co-located data from the Visible IR scanner (VIRS) and CERES (TRMM) satellites, observational estimates of SW aerosol forcing at TOA were made in 1998 during a biomass-burning episode in central America [*Christopher et al.*, 2000]. They observed an average aerosol optical depth of 1.2 with single-scattering albedo

of $\sim$0.86. Both TARFOX and ACE-2 reported a fairly wide range of values for single-scattering albedo at mid-visible wavelengths in the range of 0.85 to 0.99 for the marine aerosol impacted by continental pollution. *Sakerin and Kabanov* [2002] reported aerosol optical depth measurements over the Atlantic Ocean during the period 1989 to 1996 using shipboard expeditions. They observed aerosol optical depths in the range 0.08 to 0.38 and Angstrom wavelength exponent in the range of 0.3 to 1.1.

[21] Clear-sky aerosol surface forcing reported was about −26 W m$^{-2}$ for Atlantic Ocean during TARFOX [*Hignett et al.*, 1999] and −29 W m$^{-2}$ for tropical Indian Ocean during INDOEX [*Satheesh and Ramanathan*, 2000]. Using measurements during 1996 cruise of ORV *Sagar Kanya* and island experiments, *Jayaraman et al.* [1998] have reported aerosol forcing efficiency (visible region) of −40 W m$^{-2}$
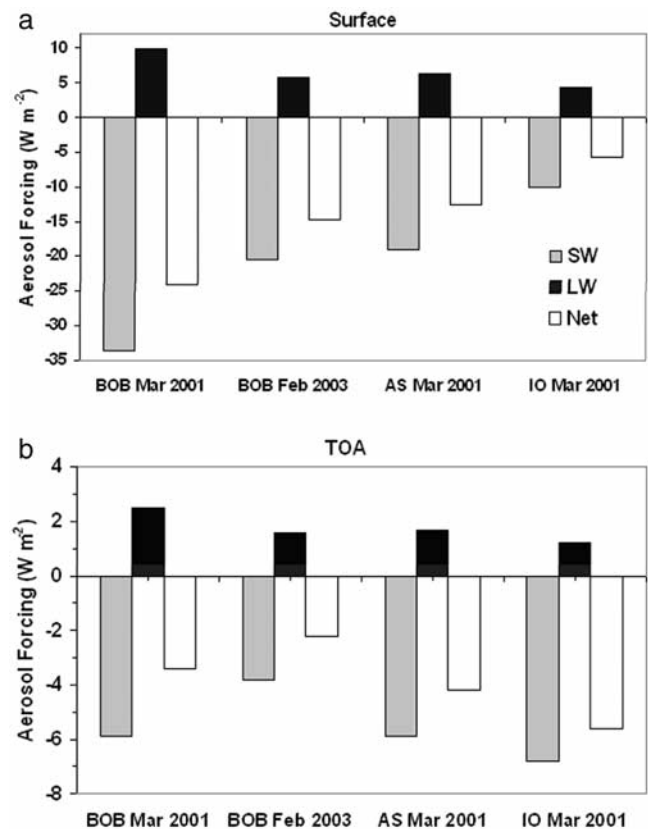


**Figure 10.** (a) Regionally averaged aerosol forcing (shortwave, longwave, and net) at the surface during different seasons and locations. (b) Regionally averaged aerosol forcing (shortwave, longwave, and net) at the top of the atmosphere during different seasons and locations.

over tropical Indian Ocean, which when multiplied with the modeled ratio of $\sim$1.73 for the SW/visible forcing efficiency, translates to $-69$ W m$^{-2}$. Using simultaneous data from MODIS and CERES observations, *Christopher et al.* [2002] have reported average value of top of the atmosphere aerosol forcing over oceans as $-6$ W m$^{-2}$. Aerosol radiative impact at the surface was studied using AERONET data in Brazil; Saharan dust in Cape Verde; and urban-industrial pollution in Creteil, near Paris, France, and near Washington, D. C. [*Kaufman et al.*, 2002]. The measured 24-h average aerosol impact on the solar flux at the surface per unit optical thickness is $-80$ W m$^{-2}$ in these sites, almost independent of the aerosol type: smoke, dust, or urban-industrial pollution [*Kaufman et al.*, 2002]. A field experiment, conducted to quantify aerosol direct radiative forcing in the southeastern United States (North Carolina) and at an adjacent valley site during June 1995 to mid-December 1995, has shown the mean cloud-free 24-h averaged aerosol forcing at the TOA (at the surface) for highly polluted, marine and continental air masses to be $-8 \pm 4$ ($-33 \pm 16$), $-7 \pm 4$ ($-13 \pm 8$), and $-0.14 \pm 0.05$ ($-8 \pm 3$) W m$^{-2}$, respectively [*Yu et al.*, 2001].

[22] Thus the above discussions show that average aerosol optical depth and aerosol forcing over Bay of Bengal are larger than that averaged over global oceans (including pristine and vast southern hemispheric oceans) and comparable to those of oceanic regions adjacent to industrialized continents (such as northern Atlantic, Mediterranean, eastern Pacific etc).

## 5. Conclusions

[23] 1. Aerosol visible optical depths over Bay of Bengal were as high as $\sim$0.6 with aerosol single-scattering albedo of $\sim$0.88 (corresponding to an aerosol black carbon fraction of $\sim$5.8%) and Angstrom wavelength exponent of $\sim$1.1, indicating the presence of a significant amount of submicron absorbing aerosols.

[24] 2. Comparison of measured aerosol optical depths using ground-based Sun photometers and MWR with those derived from MODIS (on board the TERRA platform) showed a very good agreement; both on a day-to-day basis as well as on an average with a mean difference of $\sim$0.01 and root-mean-square difference of $\sim$0.03. Such an intercomparison is done for the first time over oceanic regions adjacent to the Indian region.

[25] 3. Regionally averaged aerosol (net) forcing over Bay of Bengal was in the range $-15$ to $-24$ W m$^{-2}$ at the surface and $-2$ to $-4$ W m$^{-2}$ at the top of the atmosphere, leading to an atmospheric absorption of 13 to 20 W m$^{-2}$.

[26] 4. The aerosol forcing observed over the Bay of Bengal during February 2003 is generally smaller than the values observed over the near coastal regions of BoB during March 2001 and larger than that observed over Arabian Sea and Indian Ocean. This difference is attributed to large spread of higher AODS that prevailed in 2001.

[27] 5. The atmospheric heating due to Bay of Bengal aerosol absorption is $\sim$0.5°K/d.

## References

Angstrom, A. (1964), Techniques of determining the turbidity of the atmosphere, *Tellus*, 13, 214.

Ansmann, A., F. Wagner, D. Müller, D. Althausen, A. Herber, W. von Hoyningen-Huene, and U. Wandinger (2002), European pollution outbreaks during ACE 2: Optical particle properties inferred from multiwavelength lidar and star-Sun photometry, *J. Geophys. Res.*, 107(D15), 4259, doi:10.1029/2001JD001109.

Asnani, G. C. (1993), *Tropical Meteorology*, vols. 1 and 2, 1012 pp., Indian Inst. of Trop. Meteorol., Pashan.

Babu, S. S., and K. K. Moorthy (2001), Anthropogenic impact on aerosol black carbon mass concentration at a tropical coastal station: A case study, *Current Sci.*, 81, 1208–1214.

Babu, S. S., and K. K. Moorthy (2002), Aerosol black carbon over a tropical coastal station in India, *Geophys. Res. Lett.*, 29(23), 2098, doi:10.1029/2002GL015662.

Babu, S. S., S. K. Satheesh, and K. K. Moorthy (2002), Aerosol radiative forcing due to enhanced black carbon at an urban site in India, *Geophys. Res. Lett.*, 29(18), 1880, doi:10.1029/2002GL015826.

Bates, T. S., et al. (1998), International Global Atmospheric Chemistry (IGAC) Project's First Aerosol Characterization Experiment (ACE 1): Overview, *J. Geophys. Res.*, 103, 16,297–16,318.

Boucher, O., and D. Tanre (2000), Estimation of the aerosol perturbation to the Earth's radiative budget over oceans using POLDER satellite aerosol retrievals, *Geophys. Res. Lett.*, 27(8), 1103–1106.

Boucher, O., et al. (1998), Intercomparison of models representing direct shortwave radiative forcing by sulfate aerosols, *J. Geophys. Res.*, 103, 16979–16998.

Charlson, R. J., J. Langner, H. Rodhe, C. B. Leovy, and S. G. Warren (1991), Perturbation of the Northern Hemisphere radiative balance by backscattering from anthropogenic sulfate aerosols, *Tellus, Ser. AB*, 43, 152–163.

Charlson, R. J., S. E. Schwartz, J. M. Hales, R. D. Cess, J. A. Coakley, J. E. Hansen, and D. J. Hoffmann (1992), Climate forcing by anthropogenic aerosols, *Science*, 255, 423–430.

Christopher, S. A., J. Chou, J. L. Zhang, X. Li, T. A. Berendes, and R. M. Welch (2000), Short wave direct radiative forcing of biomass burning aerosols estimated using VIRS and CERES data, *Geophys. Res. Lett.*, 27(15), 2197–2200.

Christopher, S. A., J. Zhang, B. N. Holben, and S. K. Yang (2002), GOES-8 and NOAA-14 AVHRR retrieval of smoke aerosol optical thickness during SCAR-B, *Int. J. Remote Sens.*, 23(22), 4931–4944.

Coakley, J. A., and R. D. Cess (1985), Response of the NCAR community climate model to the radiative forcing by the naturally-occurring tropospheric aerosol, *J. Atmos. Sci.*, 42, 1677–1692.

Coakley, J. A., R. D. Cess, and F. B. Yurevich (1983), The effect of tropospheric aerosols on the Earth's radiation budget: A parameterization for climate models, *J. Atmos. Sci.*, 40, 116–138.

Das, P. K. (1986), The monsoons, 5th IMO lecture, *WMO Publ. 613*, World Meteorol. Organ., Geneva.

Eck, T. F., et al. (2001), Column-integrated aerosol optical properties over the Maldives during the northeast monsoon for 1998–2000, *J. Geophys. Res.*, 106, 28,555–28,566.

Hansen, A. D. A. (1996), Magee Scientific aethalometer user's guide, 56 pp., Magee Sci. Co., Berkeley, Calif.

Hansen, A. D. A., H. Rosen, and T. Novakov (1984), The aethalometer, an instrument for the real-time measurement of optical absorption by aerosol particles, *Sci. Total Environ.*, 36, 191–196.

Hansen, J. E., M. Sato, A. Lacis, R. Ruedy, I. Tegen, and E. Matthews (1998), Climate forcings in the industrial era, *Proc. Natl. Acad. Sci. U. S. A.*, 95(22), 12,753–12,758.

Haywood, J. M., V. Ramaswamy, and B. J. Soden (1999), Tropospheric aerosol climate forcing in clear-sky satellite observations over the oceans, *Science*, 283, 1299–1303.

Hess, M., P. Koepke, and I. Schult (1998), Optical properties of aerosols and clouds: The software package OPAC, *Bull. Am. Meteorol. Soc.*, 79, 831–844.

Hignett, P., J. P. Taylor, P. N. Francis, and M. D. Glew (1999), Comparison of observed and modeled direct aerosol forcing during TARFOX, *J. Geophys. Res.*, 104, 2279–2287.

Ichoku, C., et al. (2002a), Analysis of the performance characteristics of the five-channel Microtops II Sun photometer for measuring aerosol optical thickness and precipitable water vapor, *J. Geophys. Res.*, 107(D13), 4179, doi:10.1029/2001JD001302.

Ichoku, C., D. A. Chu, S. Chu, Y. J. Kaufman, L. A. Remer, D. Tanré, I. Slutsker, and B. N. Holben (2002b), A spatio-temporal approach for global validation and analysis of MODIS aerosol products, *Geophys. Res. Lett.*, 29(12), 8006, doi:10.1029/2001GL013206.

Intergovernmental Panel on Climate Change (2001), *Climate Change 1994: Radiative Forcing of Climate, Report to IPCC From the Scientific Assessment Group (WGI)*, Cambridge Univ. Press, New York.

Jayaraman, A., D. Lubin, S. Ramachandran, V. Ramanathan, E. Woodbridge, W. Collins, and K. S. Zalpuri (1998), Direct observations of aerosol radiative forcing over the tropical Indian Ocean during the January-February 1996 pre-INDOEX cruise, *J. Geophys. Res.*, 103, 13,827–13,836.

Kaufman, Y. J., et al. (1998), Smoke, Clouds, and Radiation-Brazil (SCAR-B) experiment, *J. Geophys. Res.*, 103, 31,783–31,808.

Kaufman, Y. J., D. Tanre, B. N. Holben, S. Mattoo, L. A. Remer, T. F. Eck, J. Vaughan, and B. Chatenet (2002), Aerosol radiative impact on spectral solar flux at the surface, derived from principal-plane sky measurements, *J. Atmos. Sci.*, 59, 635–646.

Kaufman, Y. J., et al. (2003), Fire and smoke observed from the Earth Observing System MODIS instrument: Products, validation, and operational use, *Int. J. Remote Sens.*, 24(8), 1765–1781.

Li, F., and V. Ramanathan (2002), Winter to summer monsoon variation of aerosol optical depth over the tropical Indian Ocean, *J. Geophys. Res.*, 107(D16), 4284, doi:10.1029/2001JD000949.

Liou, K. N. (1980), *An Introduction to Atmospheric Radiation*, 392 pp., Harcourt Brace Jovanovich, Academic, San Diego, Calif.

Moorthy, K. K., and S. K. Satheesh (2000), Characteristics of aerosols over a remote island, Minicoy in the Arabian Sea: Optical properties and retrieved size characteristics, *Q. J. R. Meteorol. Soc.*, 126, 81–109.

Moorthy, K. K., S. K. Satheesh, and B. V. K. Murthy (1997), Investigations of marine aerosols over tropical Indian Ocean, *J. Geophys. Res.*, 102, 18,827–18,842.

Moorthy, K. K., S. K. Satheesh, and B. V. K. Murthy (1998), Characteristics of spectral optical depths and size distributions of aerosols over tropical oceanic regions, *J. Atmos. Sol. Terr. Phys.*, 60(10), 981–992.

Moorthy, K. K., et al. (1999), Aerosol climatology over India: 1. ISRO GBP MWR network and database, *ISRO GBP SR-03-99*, Indian Space Res. Organ., Bangalore.

Moorthy, K. K., et al. (2001), Aerosol optical depths over peninsular India and adjoining oceans during the INDOEX campaigns: Spatial, temporal, and spectral characteristics, *J. Geophys. Res.*, 106, 28,539–28,554.

Moorthy, K. K., S. S. Babu, and S. K. Satheesh (2003), Aerosol spectral optical depths over the Bay of Bengal: Role of transport, *Geophys. Res. Lett.*, 30(5), 1249, doi:10.1029/2002GL016520.

Morys, M., F. M. Mims III, S. Hagerup, S. E. Anderson, A. Baker, J. Kia, and T. Walkup (2001), Design, calibration and performance of Microtops II handheld ozone monitor and Sun photometer, *J. Geophys. Res.*, 106, 14,573–14,582.

Nemesure, S., R. Wagener, and S. E. Schuartz (1995), Direct shortwave forcing of climate by the anthropogenic sulfate aerosol: Sensitivity to particle size, composition, and relative humidity, *J. Geophys. Res.*, 100, 26,105–26,116.

Pillai, P. S., and K. K. Moorthy (2001), Aerosol mass-size distributions at a tropical coastal environment: Response to measoscale and synoptic processes, *Atmos. Environ.*, 35, 4099–4112.

Porter, J. N., M. Miller, C. Pietras, and C. Motell (2001), Ship based Sun photometer measurements using Microtops Sun photometer, *J. Atmos. Oceanic Technol.*, 18, 744–765.

Raes, F. (1995), Entrainment of free tropospheric aerosols as a regulating mechanism for cloud condensation nuclei in the remote marine boundary layer, *J. Geophys. Res.*, 100, 2893–2903.

Ramanathan, V., et al. (2001), Indian Ocean Experiment: An integrated analysis of the climate forcing and effects of the great Indo-Asian haze, *J. Geophys. Res.*, 106, 28,371–28,398.

Remer, L. A., et al. (2002), Validation of MODIS aerosol retrieval over ocean, *Geophys. Res. Lett.*, 29(12), 8008, doi:10.1029/2001GL013204.

Ricchiazzi, P., S. Yang, C. Gautier, and D. Sowle (1998), SBDART, A research and teaching tool for plane-parellel radiative transfer in the Earth's atmosphere, *Bull. Am. Meteorol. Soc.*, 79, 2101–2114.

Russell, P. B., P. V. Hobbs, and L. L. Stowe (1999), Aerosol properties and radiative effects in the United States East Coast haze plume: An overview of the Tropospheric Aerosol Radiative Forcing Observational Experiment (TARFOX), *J. Geophys. Res.*, 104, 2213–2222.

Sakerin, S. M., and D. M. Kabanov (2002), Spatial inhomogeneities and the spectral behavior of atmospheric aerosol optical depth over the Atlantic Ocean, *J. Atmos. Sci.*, 59, 484–500.

Satheesh, S. K. (2002), Radiative forcing by aerosols over Bay of Bengal region, *Geophys. Res. Lett.*, 29(22), 2083, doi:10.1029/2002GL015334.

Satheesh, S. K., and K. K. Moorthy (1997), Aerosol characteristics over coastal regions of the Arabian Sea, *Tellus, Ser. B*, 49, 417–428.

Satheesh, S. K., and V. Ramanathan (2000), Large differences in the tropical aerosol forcing at the top of the atmosphere and Earth's surface, *Nature*, 405, 60–63.

Satheesh, S. K., and J. Srinivasan (2002), Enhanced aerosol loading over Arabian Sea during the pre-monsoon season: Natural or anthropogenic?, *Geophys. Res. Lett.*, 29(18), 1874, doi:10.1029/2002GL015687.

Satheesh, S. K., V. Ramanathan, X. L. Jones, J. M. Lobert, I. A. Podgorny, J. M. Prospero, B. N. Holben, and N. G. Loeb (1999), A model for the natural and anthropogenic aerosols for the tropical Indian Ocean derived from Indian Ocean Experiment data, *J. Geophys. Res.*, 104, 27,421–27,440.

Satheesh, S. K., K. K. Moorthy, and I. Das (2001), Aerosol spectral optical depths over Bay of Bengal, Indian Ocean and Arabian Sea, *Current Sci.*, 81, 1617–1625.

Shaw, G. E., J. A. Regan, and B. M. Herman (1973), Investigations of atmospheric extinction using direct solar radiation measurements made with a multiple wavelength radiometer, *J. Appl. Meteorol.*, 12, 374–380.

Smirnov, A., et al. (1995), Aerosol optical depths over oceans: Analysis in terms of synoptic airmass types, *J. Geophys. Res.*, 100, 16,639–16,650.

Smirnov, A., B. N. Holben, O. Dubovik, N. T. O'Neill, L. A. Remer, T. F. Eck, I. Slutsker, and D. Savoie (2000), Measurement of atmospheric optical parameters on US Atlantic coast sites, ships, and Bermuda during TARFOX, *J. Geophys. Res.*, 105, 9887–9901.

Smirnov, A., B. N. Holben, O. Dubovik, N. T. O'Neill, T. F. Eck, D. L. Westphal, A. K. Goroch, C. Pietras, and I. Slutsker (2002), Atmospheric aerosol optical properties in the Persian Gulf, *J. Atmos. Sci.*, 59, 620–634.

Soden, B., et al. (2000), An intercomparison of radiation codes for retrieving upper-troposphere humidity in the 6.3-μm band: A report from the first GVaP workshop, *Bull. Am. Meteorol. Soc.*, 81, 797–808.

Subbaraya, B. H., A. Jayaraman, K. K. Moorthy, and M. Mohan (2000), Atmospheric aerosol studies under ISRO's Geosphere Biosphere Programme, *J. Indian Geophys. Union*, 4, 77–90.

Yu, S. C., V. K. Saxena, and Z. C. Zhao (2001), A comparison of signals of regional aerosol-induced forcing in eastern China and the southeastern United States, *Geophys. Res. Lett.*, 28(4), 713–716.

---

S. S. Babu and K. K. Moorthy, Space Physics Laboratory, Vikram Sarabhai Space Centre, Thiruvananthapuram 695 022, India.

Y. J. Kaufman, Climate and Radiation Branch, NASA Goddard Space Flight Center, Code 913, Building 33, Room A308, Greenbelt, MD 20771, USA.

S. K. Satheesh and V. Vinoj, Centre for Atmospheric and Oceanic Sciences, Indian Institute of Science, Bangalore 560 012, India. (satheesh@caos.iisc.ernet.in)